A study on parameter estimation and suppression for smeared spectrum jamming based on short-time Fourier transform

Chuanzhang Wu[†], Baixiao Chen[*†] 🆔, Minglei Yang and Mei Dong

*Correspondence:
bxchen@xidian.edu.cn
[†]Chuanzhang Wu and Baixiao Chen
contributed equally to this work.
National Laboratory of Radar Signal
Processing, Xidian University, No.2
Taibai South Road, 710071 Xi'an,
China

Abstract

We address the suppressing problem of smeared spectrum (SMSP) jamming from the mixed signal received by the radar. To this end, we resort to the time-frequency analysis algorithm and give the concrete expression formula of the short-time Fourier transform (STFT) of SMSP jamming. The proposed method is to estimate the parameters of the jamming signal based on the STFT result, and then the jamming signal is reconstructed and suppressed form the mixed signal. In order to perform effective interference even after the pulse compression process, the jamming-to-target ratio (JSR) is always positive. Based on this assumption, the estimation steps for different parameters of SMSP jamming are given, including the number of sub-waveforms, the amplitude, and the time delay. The influence of choosing different window is also considered in this paper. The estimated performance of this method is verified by Monte Carlo simulation, and the results show the effectiveness of the proposed method.

Keywords: Smeared spectrum, Short-time Fourier transform, Parameter estimation, Signal reconstruction, Jamming cancellation

1   Introduction

For a long time, the linear frequency modulation (LFM) signal plays a vital role in modern radar system. As a kind of pulse compressed signal, it is insensitive to Doppler shift and has a low probability of being intercepted. In order to counter this kind of signals, Sparrow and Cikalo [1] proposed a new interfere strategy in 2006, which is named smeared spectrum (SMSP) jamming. After being captured, the incoming signal is compressed in time domain, and then repeated for several times to maintain the time width of signal unchanged. As a result, the SMSP jamming has high similarity to target echo, and could form a large number of false targets with a shape of comb after pulse compression processing. It makes it difficult for radar to detect true targets and even makes the radar system ineffective.

Along with the development of digital radio frequency memory (DRFM) technique, the SMSP approach is getting more and more mature. However, there is an increasing

concern over its recognition and suppression problems by many researchers. Essentially, the chirp rate is the greatest difference between SMSP jamming and target echo and is usually used in interference identification. In [2] and [3], the authors separately utilized the matched signal transform and the fractional power spectrum to recognize the SMSP jamming from the target signal according to their difference in chirp rate. Similarly, the SMSP jamming is recognized by peak detection in the distance dimensionality of the discrete match Fourier transform result in [4]. In [5] and [6], the authors respectively analyzed the features of SMSP jamming from the aspects of the ambiguity function, the magnitude spectrum and the frequency spectrum, and extracted these features to distinguish SMSP jamming and target echo. In [7] and [8], Ding separately used the basis pursuit method and the sparse decomposition algorithm to reconstruct signal and identified SMSP jamming by the difference of the chirp rate.

In the study of SMSP jamming suppression, the existing methods can be divided into two categories[9–12], jamming reconstruction and signal filtering. The jamming reconstruction method actually contains two parts, jamming signal reconstruction by estimating different parameters of jamming and jamming cancellation. On the other side, the signal filtering method is achieved by transforming the jamming signal into other domain and designing a proper filter to suppress it. Sun [9] proposed the methods to counter SMSP jamming from three aspects, fractional Fourier transform, Fourier transform, and atom decomposition, and all of these methods showed good performance. In [10], Li suppressed the SMSP jamming by estimating its different parameters. However, this method may become invalid in low jamming-to-noise ratio (JNR) scenario, because its time delay is directly estimated by finding the position where the amplitude hops in the time domain of the received signal. By contrast, the estimation method to time delay given in [11] showed stronger robustness by searching it within a detecting window. In [12], authors firstly abandoned the jamming signal in time-frequency domain, and then recovered the losing target signal by compressed sensing algorithm. Although this method can totally suppress jamming signal, it suffers from a huge computational burden. Different with these methods, Lu [13] regarded the jamming signal as a kind of range false targets and suppressed it through pulse diversity, while it had a performance loss.

Motivated by the huge difference between SMSP jamming and target echo in time-frequency domain, we propose a parameter estimation method based on short-time Fourier transform (STFT).

Comparing with other time-frequency analysis methods, like Gabor transform [14] and Wigner-Ville distribution (WVD) [15], STFT have a simpler form and is easier to derive. Moreover, it does not occur cross term [16]. As a kind of linear time-frequency representation method, the STFT algorithm is widely applied in medicine, optics, and many other aspects [17–20]. In this paper, we focus on analyzing the STFT result of the mixed signal and use it to estimate all parameters of jamming signal.

This paper is organized as follows. Section 2 will introduce the signal model of SMSP jamming. In Section 3, we derive mathematical expression of STFT result in detail. Section 4, we will give the detailed steps to estimate different parameters of jamming signal. Simulation results and the comparison result with other method are shown in Section 5. Finally the conclusions are given in Section 6.

2   Signal models

After capturing the transmitted signal from radar, the jammer uses an A/D converter with a clock l to store it. Once being recalled, the stored digital signal is converted into analog signal by a D/A converter with a clock Ml. Repeat these converting steps for M times, and the SMSP jamming is generated [1].

Assume that the pulse Doppler radar transmits a baseband LFM signal

$$s(t) = \exp\left(j\pi\mu t^2\right), \ \mu = B/T, \ 0 \le t \le T \tag{1}$$

where μ denotes the chirp rate, and B and T represent the bandwidth and the pulse duration of transmitted signal, respectively.

According to the process of producing the SMSP jamming, it is composed of M identical sub-waveforms. Each of them is an LFM signal with bandwidth B and pulse duration $T_J = T/M$, which results in its chirp rate is M times of the captured signal. Then, the mth sub-waveform of SMSP jamming can be formulated as [1]

$$\begin{aligned} J^{(m)}(t) &= A_J\exp\left(j\pi\mu'(t - mT_j)^2\right) \\ &\approx A_J\exp\left[j\pi\left(\mu't^2 - 2mBt\right)\right] \\ &mT_J \le t \le (m+1)T_J \end{aligned} \tag{2}$$

where A_J denotes the complex envelope of jamming signal, and $\mu' = B/T_J = M\mu$ denotes its chirp rate. In (2), we ignore the constant phase item that is independent of t. Thus, the SMSP jamming signal can be written as

$$J_{\text{SMSP}}(t) = \sum_{m=0}^{M-1} J^{(m)}(t) \tag{3}$$

Figure 1 shows the time domain of the SMSP signal. Due to the similarity in the signal's form and the difference in chirp rate to the transmitted signal from radar, the SMSP jamming can also obtain certain gain after pulse compression process. What is worse, it

Fig. 1 The time domain of SMSP jamming (B=15MHz, T=10us, M=5)
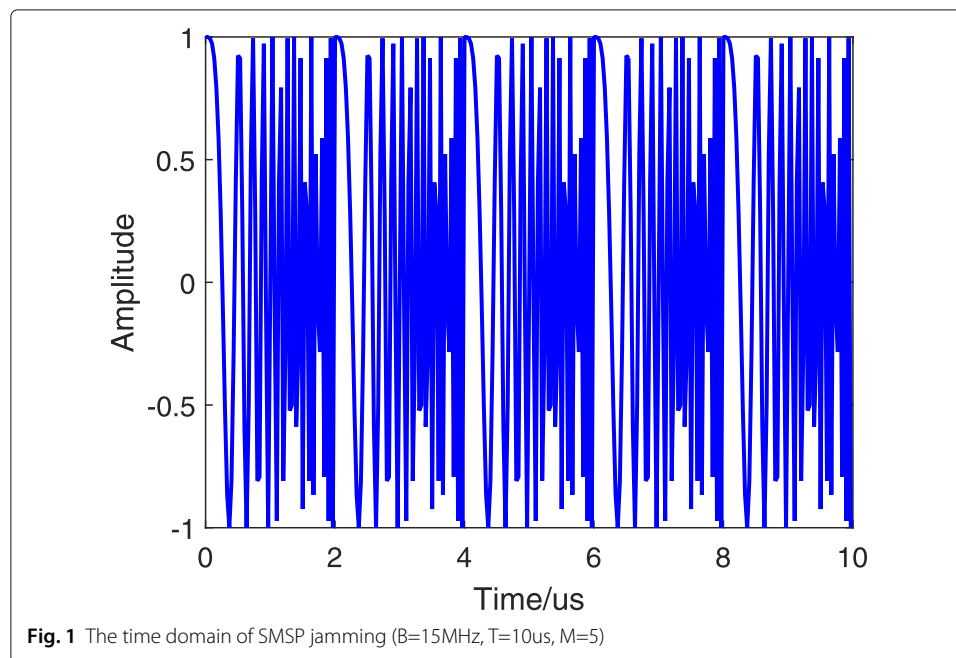
can form plenty of false targets surrounding around the true target, which causes great difficulty for radar to detect the real target.

As the LFM signal is not sensitive to Doppler frequency, the velocity of the jamming signal is not considered here [11, 12]. Interfered by SMSP jamming, the mixed signal that was received by radar is written as follows

$$y(t) = A_T s(t - \tau_t) + J_{\text{SMSP}}(t - \tau_J) + n(t) \tag{4}$$

where A_T denotes the complex envelope of target echo, τ_t and τ_J represent the time delay of target echo and SMSP jamming respectively, and $n(t)$ denotes the white Gaussian noise. In the following content, the signal-to-noise ratio (SNR) is defined as $SNR = A_T^2/\sigma_n^2$, and the jamming-to-signal ratio (JSR) is defined as $JSR = A_J^2/A_T^2$, where σ_n^2 is the power of the noise.

3   The STFT of SMSP

The short-time Fourier transform divides a longer time signal into many shorter segments of equal length, and then computes the Fourier transform separately on each segments [16]. It reveals the local time-frequency characteristics of signal.

Let $h(t)$ be a narrow analysis window in time domain. Then, for an analog signal $z(t)$, its STFT is defined as

$$\text{STFT}(t,f) = \int_{-\infty}^{\infty} z(u) h^*(u - t) e^{-j2\pi fu} du \tag{5}$$

where $(\cdot)^*$ stands for the conjugate operator.

Without loss of generality, we assume that the window function $h(t)$ is rectangular with length t_L, i.e.,

$$h(t) = \begin{cases} 1, \ 0 \leq t \leq t_L \\ 0, \ \text{else} \end{cases} \tag{6}$$

Generally speaking, the length of the window should not be too large to sufficiently obtain the local features of the signal, or it does not exceed the time width of the sub-waveform, i.e., $t_L < T_J$.

Figure 2 illustrates the time-frequency characteristic of LFM signal and SMSP jamming. It can be seen that the STFT of jamming signal should be discussed in two scenarios according to the position of the analysis window, i.e., the window within a single sub-waveform and the window across two sub-waveforms. We respectively denote the corresponding STFT results as $\text{STFT}_1(t,f)$ and $\text{STFT}_2(t,f)$.

3.1   Window within single sub-waveform

As is shown in the second plot of Fig. 2, when the analysis window is located in single sub-waveform, the extracted signal is also an LFM signal with time duration t_L and bandwidth $\mu' t_L$.

Assume the analysis window is located within the mth sub-waveform. Then, the STFT of jamming signal by this time is equivalent to the Fourier transform of the extracted LFM signal [21] and can be calculated as follows
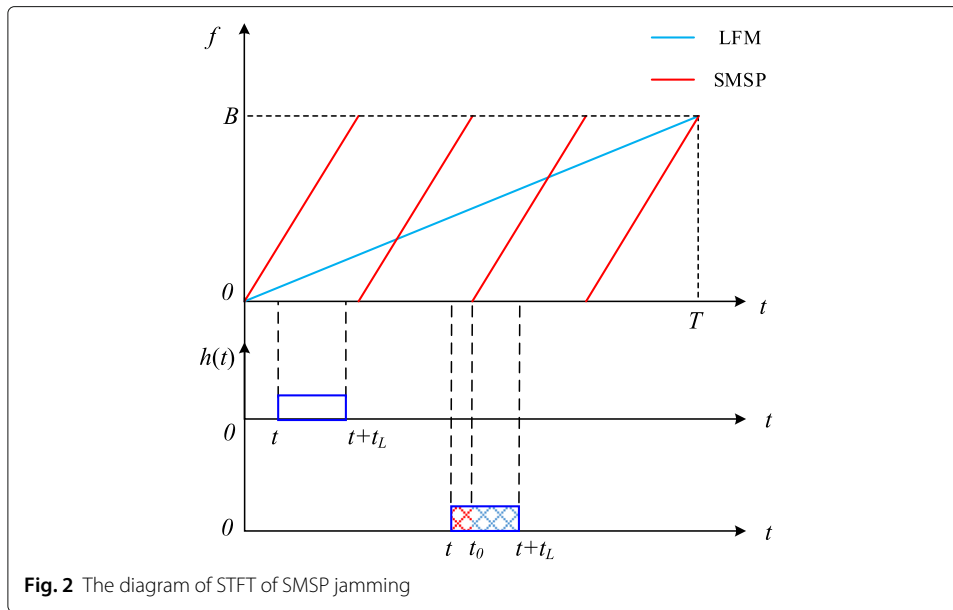
Fig. 2 The diagram of STFT of SMSP jamming

$$
\begin{aligned}
\mathrm{STFT}_1(t,f) &= \int_{-\infty}^{\infty} J^{(m)}(u) h^*(u-t) e^{-j2\pi fu} du \\
&= \int_{t}^{t+t_L} A_J e^{j\pi(\mu' u^2 - 2mBu)} e^{-j2\pi fu} du \\
&= A_J e^{-\frac{j\pi(f+mB)^2}{\mu'}} \int_{t}^{t+t_L} e^{j(\pi/2)2\mu'\left(u - \frac{f+mB}{\mu'}\right)^2} du
\end{aligned}
\tag{7}
$$

Let

$$
v = \sqrt{2\mu'}\left(u - \frac{f+mB}{\mu'}\right)
\tag{8}
$$

and perform the variable substitution. Then, (7) is rewritten as

$$
\begin{aligned}
\mathrm{STFT}_1(t,f) &= \frac{A_J}{\sqrt{2\mu'}} e^{-\frac{j\pi(f+mB)^2}{\mu'}} \int_{v1}^{v2} e^{j\pi v^2/2} dv \\
&= \frac{A_J}{\sqrt{2\mu'}} e^{-\frac{j\pi(f+mB)^2}{\mu'}} \\
&\quad \cdot \left[\int_{v1}^{v2} \left(\cos\frac{\pi v^2}{2} + j\sin\frac{\pi v^2}{2} \right) dv \right]
\end{aligned}
\tag{9}
$$

where

$$
\begin{aligned}
v_1 &= \sqrt{2\mu'}\left(t - \frac{f+mB}{\mu'}\right) \\
v_2 &= \sqrt{2\mu'}\left(t - t_L - \frac{f+mB}{\mu'}\right) \\
&= v_1 + \sqrt{2\mu'} t_L
\end{aligned}
\tag{10}
$$

The Fresnel integrals, denoted by $C(v)$ and $S(v)$, are defined by

$$
\begin{aligned}
C(v) &= \int_{0}^{v} \cos\left(\frac{\pi x^2}{2}\right) dx \\
S(v) &= \int_{0}^{v} \sin\left(\frac{\pi x^2}{2}\right) dx
\end{aligned}
\tag{11}
$$

Let

$$F(v) = [C(v + \sqrt{2\mu'}t_L) - C(v)] + j[S(v + \sqrt{2\mu'}t_L) - S(v)], \tag{12}$$

and then (9) can be further rewritten as

$$\text{STFT}_1(t,f) = \frac{A_J}{\sqrt{2\mu'}} e^{-\frac{j\pi(f+mB)^2}{\mu'}} F(v_1) \tag{13}$$

The amplitude of (13) is

$$|\text{STFT}_1(t,f)| = \frac{A_J}{\sqrt{2\mu'}} |F(v_1)| \tag{14}$$

Obviously, once the window function and the chirp rate μ' of SMSP jamming are priori known, $\sqrt{2\mu'}t_L$ can be easy to be calculated. Then, we can obtain the maximum value of $|F(v_1)|$ and further get the maximum value of $|\text{STFT}_1(t,f)|$.

In fact, the real part and the imaginary part of $F(v)$ can be separately seen as the slope of the line between two points with fixed interval $\sqrt{2\mu'}t_L$ in $C(v)$ and $S(v)$. According to the functional properties of $C(v)$ and $S(v)$ and our experiment results, the value of $|F(v_1)|$ maximizes when these two points are symmetric around the origin, which means $v_1 = -\sqrt{2\mu'}t_L/2$. Substitute this equation into (10), we have

$$\sqrt{2\mu'}\left(t - \frac{f+mB}{\mu'}\right) = -\frac{\sqrt{2\mu'}t_L}{2} \tag{15}$$

Thus, in each discrete frequency channel $f = lf_s/L$, the time at which the local maximum amplitude is located is

$$t_{\max} = \frac{lf_s}{\mu'L} - \frac{t_L}{2} + mT_j \tag{16}$$

where L denotes the total number of frequency channels, and $l = 0, 1, \cdots, L-1$.

3.1.1 Window across two sub-waveforms

As is shown in the third plot of Fig. 2, the extracted signal segment includes two parts when the analysis window spans two sub-waveforms, which are shown with red grid lines and blue grid lines respectively.

Assume that the indexes of sub-waveforms that the analysis window spanned are m and $m + 1$. It means that the window is located around the time $t_0 = mT_j$. Then, the STFT of jamming signal by this time is calculated by

$$\begin{aligned}
\text{STFT}_2(t,f) &= \int_{-\infty}^{\infty} J^{(m)}(u)h^*(u-t)e^{-j2\pi fu}du \\
&= \int_t^{t_0} A_J e^{j\pi(\mu'u^2 - 2mBu)} e^{-j2\pi fu}du \\
&\quad + \int_{t_0}^{t+t_L} A_J e^{j\pi[\mu'u^2 - 2(m+1)Bu]} e^{-j2\pi fu}du \\
&= A_J\left[\int_t^{t_0} e^{j\varphi_1(u)}du + \int_{t_0}^{t+t_0} e^{j\varphi_2(u)}du\right]
\end{aligned} \tag{17}$$

where $\varphi_1(u) = \pi\mu'u^2 - 2\pi(f+mB)u$ and $\varphi_2(u) = \pi\mu'u^2 - 2\pi[f+(m+1)B]u$.

In order to obtain an approximate result about (17), we resort to the Euler's formula and divided each of them into real part and imaginary part. For the first component in the fourth line of (17), we have

$$\int_t^{t_0} e^{j\varphi_1(u)} du$$
$$= \int_t^{t_0} \cos(\varphi_1(u)) du + j \int_t^{t_0} \sin(\varphi_1(u)) du \qquad (18)$$
$$= P_1 + jP_2$$

As P_1 and P_2 is the integral of a cosine function around t_0, it can be approximated by Taylor series expansion. Let $A_1 = 2\pi\mu' t_0 - 2\pi(f + mB)$, then

$$\cos(\varphi_1(u)) \approx \cos(\varphi_1(t_0)) - A_1 \sin(\varphi_1(t_0))(u - t_0)$$
$$\sin(\varphi_1(u)) \approx \sin(\varphi_1(t_0)) + A_1 \cos(\varphi_1(t_0))(u - t_0) \qquad (19)$$

Substitute (19) into (18), P_1 and P_2 can be rewritten as

$$P_1 = (t_0 - t)\cos(\varphi_1(t_0)) + A_1 t_0(t_0 - t)\sin(\varphi_1(t_0))$$
$$\quad - A_1 \sin(\varphi_1(t_0)) \frac{t_0^2 - t^2}{2}$$
$$P_2 = (t_0 - t)\sin(\varphi_1(t_0)) - A_1 t_0(t_0 - t)\cos(\varphi_1(t_0)) \qquad (20)$$
$$\quad + A_1 \cos(\varphi_1(t_0)) \frac{t_0^2 - t^2}{2}$$

Similarly, for the second component in (17), let $A_2 = 2\pi\mu' t_0 - 2\pi[f + (m+1)B]$, and we have

$$P_3 = \int_{t_0}^{t+t_L} \cos(\varphi_2(u)) du$$
$$= (t + t_L - t_0)\cos(\varphi_2(t_0))$$
$$\quad + A_2 t_0(t + t_L - t_0)\sin(\varphi_2(t_0))$$
$$\quad - A_2 \sin(\varphi_2(t_0)) \frac{(t + t_L)^2 - t_0^2}{2}$$
$$P_4 = \int_{t_0}^{t+t_L} \sin(\varphi_2(u)) du \qquad (21)$$
$$= (t + t_L - t_0)\sin(\varphi_2(t_0))$$
$$\quad - A_2 t_0(t + t_L - t_0)\cos(\varphi_2(t_0))$$
$$\quad + A_2 \cos(\varphi_2(t_0)) \frac{(t + t_L)^2 - t_0^2}{2}$$

As the integral variable in (18) is around t_0, it means the frequency of the extracted signal is around B, i.e. $f \approx B$ in (20). Similarly, we have $f \approx 0$ in (21). Then, it can be deduced that

$$\varphi_1(t_0) \approx \varphi_2(t_0), A_1 \approx A_2. \qquad (22)$$

Substitute (20) and (21) into (17), and use the approximation in (22), we can yield

$$\text{STFT}_2(t,f) = A_J[(P_1 + jP_2) + (P_3 + jP_4)]$$
$$= A_J\{[t_L \cos(\varphi_1(t_0)) - A_V \sin(\varphi_1(t_0))] \qquad (23)$$
$$\quad + j[t_L \sin(\varphi_1(t_0)) + A_V \cos(\varphi_1(t_0))]\}$$

where $A_V = A_1(t_L^2 + 2t_L t - 2t_0 t_L)/2$.

Mathematically, $\text{STFT}_2(t,f)$ is comprised of two orthometric vectors. Clearly, one of the vector is fixed with length $A_J t_L$, and the another one is changeable with length $A_J A_V$. When its module $|\text{STFT}_2(t,f)|$ minimizes, the vector related to t is 0, i.e.,

$$A_J A_1 \frac{t_L^2 + 2t_L t - 2t_0 t_L}{2} = 0 \tag{24}$$

thus, we have

$$t_{\min} = t_0 - \frac{t_L}{2} \tag{25}$$

Apparently, the analysis window is located in the middle of two sub-waveforms at this point. And the corresponding minimum amplitude of STFT is

$$|\text{STFT}_2(t,f)|_{\min} = A_J t_L \tag{26}$$

Combining (12) with (23), we can obtain the complete STFT of the SMSP jamming

$$\text{STFT}(t,f) = \begin{cases} \text{STFT}_1(t,f), mT_j \leq t < (m+1)T_j - t_L \\ \text{STFT}_2(t,f), nT_j - t_L \leq t < nT_j \end{cases} \tag{27}$$

where $m = 0, 1, \cdots, M-1$ and $n = 1, 2, \cdots, M-1$.

3.2 STFT with other windows

In fact, if we choose other analysis windows, the close form of the STFT result of jamming signal becomes very hard to obtain.

Let

$$h(t) = \begin{cases} g(t), \, 0 \leq t \leq t_L \\ 0, \, else \end{cases} \tag{28}$$

where $g(t)$ can be a Hamming window and Gaussian window and so on. Then, the STFT result of jamming signal can be derived by using the convolution theorem. The convolution theorem state that the filtering in time domain is equal to the convolution in frequency domain. Take the first scenario as an example, the corresponding short-time Fourier transform $\text{STFT}'_1(t,f)$ can be calculated as follows

$$
\begin{aligned}
\text{STFT}'_1(t,f) &= \int_{-\infty}^{\infty} J^{(m)}(u) h^*(u-t) e^{-j2\pi fu} du \\
&= \int_{t}^{t+t_L} J^{(m)}(u) g^*(u-t) e^{-j2\pi fu} du \\
&= \frac{1}{N} \left[\int_{t}^{t+t_L} J^{(m)}(u) e^{-j2\pi fu} du \right] \\
&\quad \otimes G(-f) e^{-j2\pi ft} \\
&= \frac{1}{N} \text{STFT}_1(t,f) \otimes G(-f) e^{-j2\pi ft}
\end{aligned}
\tag{29}
$$

where $\otimes$ denotes the convolution operator, and $G(f)$ is the Fourier transform of $g(t)$.

From (29), $\text{STFT}'_1(t,f)$ is the convolution of $\text{STFT}_1(t,f)$ and the exponential weighted $G(-f)$. Considering that the energy of $G(f)$ is concentrated in the narrow main lobe, $\text{STFT}'_1(t_0,f)$ is actually approximated to the product of $\text{STFT}_1(t_0,f)$ and the maximum of $G(f)$ for a fixed start time t_0. As a result, the maximum value of $|\text{STFT}'_1(t,f)|$ can be approximated as the product of the maximum of $|\text{STFT}_1(t,f)|$ and the maximum of $|G(f)|$. This also hold true for the rectangular window in (7). In this case, $G(f)$ is a *sinc*

function with very narrow main lobe. The factor $\frac{1}{N}$ exists to maintain the consistency between these two equations.

The derivation of the STFT result in the second scenario is similar to this, and we do not discuss it in detail here.

4 Methods of parameter estimation and jamming reconstruct

In order to reconstruct the SMSP jamming signal and suppress it from the mixed signal, it is our priority to estimate its parameters. Parameter estimation of SMSP jamming includes three aspects: the number of sub-waveforms (or the chirp rate), the amplitude, and the time delay.

4.1 Estimation of the number of sub-waveforms

As mentioned earlier, the target echo could get larger gain after pulse compression process than that of the SMSP jamming. Therefore, the JSR in the mixed signal is always relatively great in order to achieve interference effectively even after pulse compression. Based on this assumption, the module of STFT result of the SMSP jamming is bigger than that of the target echo. Consequently, for the Fourier transform result on each signal segments, the maximum amplitude in the frequency dimension always corresponds to the jamming signal. This provides a chance for us to estimate jamming's amplitude from the mixed signal.

According to the time-frequency characteristics of the SMSP jamming as shown in Fig. 2, its frequency hops between two adjacent sub-waveforms. Based on this fact, the number of sub-waveforms can be estimated by following steps:

Step1: Calculate the STFT of the received mixed signal;

Step2: Search each time profiles, and choose the frequency channel that corresponds to the maximum modules of the Fourier transform result, i.e.,

$$\mathcal{F}(f) = \arg\max_f |\mathrm{STFT}(t,f)| \tag{30}$$

Step3: Count the number of frequency hopping $\tilde{M}$ from B to 0 in $\mathcal{F}(f)$. Then, the number of sub-waveforms is estimated as $\tilde{M}+1$, and the corresponding chirp rate of jamming signal can be estimated as $\tilde{\mu}' = (\tilde{M}+1)B/T$.

In fact, this step may become more visualized if we perform difference operation on $\mathcal{F}(f)$, and the result is the same.

4.2 Estimation of the amplitude of jamming

As mentioned in Section 2, the local maximum of $\mathrm{STFT}_1(t,f)$ is related to the value of $F(v_1)$. Considering that the maximum of $F(v_1)$ is actually the maximum of $F(v)$, the estimation to amplitude A_J of SMSP jamming can be carried out through following steps:

Step1: Construct the function $F(v)$ in (12) according to the estimated chirp rate $\tilde{\mu}'$ and the length t_L of the selected analysis window;

Step2: Obtain the maximum value of $|F(v)|$ by simulation experiment, and denote it as $F_{\max}$;

Step3: Obtain all the local maximum modules in each frequency channel within each sub-waveform $|\mathrm{STFT}|_{l\max}^{(i)}$ according to the STFT result of the mixed signal, except the ones in which SMSP jamming intersects with target echo in time-frequency domain.

Step4: Calculate the average value of $|\text{STFT}|^{(i)}_{\text{lmax}}$, i.e., $|\text{STFT}|_{\text{lmax}} = \mathbf{E}\{|\text{STFT}|^{(i)}_{\text{lmax}}\}$. Then, according to (14), the amplitude of jamming signal can be estimated as

$$\tilde{A}_J = \frac{\sqrt{2\tilde{u}'}|\text{STFT}|_{\text{lmax}}}{F_{\text{max}}} \tag{31}$$

For the scenario when a non-rectangular window is chosen, $\tilde{A}_J$ can be estimated by normalizing $\text{STFT}'(t,f)$ with the local maximum module of rectangular window's Fourier transform $G(f)$.

4.3 Estimation of the time delay of signal

Without loss of generality, we consider the scenario that the jamming signal has same time delay as the target echo, i.e. $\tau_J = \tau_t$ in (4). Actually, the estimated accuracy of time delay could greatly impact the performance of jamming reconstruction and jamming cancellation. In order to estimate the time delay more precisely, the method of combining coarse estimation and fine estimation is adopted.

Firstly, the coarse estimation algorithm is used to roughly estimate the position of the time delay. It is realized by analyzing the STFT result of SMSP jamming signal. According to the time-frequency characteristics, the time interval between two adjacent points, where SMSP jamming and target echo intersect in the time-frequency domain, is $T/(M-1)$, so does the difference between the first intersection to the time delay. However, in the STFT result of the mixed signal, the amplitude stacks up at these positions. As a result, the first intersection is located at the place where $|\text{STFT}(t,f)|$ has the first maximum value (bigger than $|\text{STFT}|^{(i)}_{\text{lmax}}$), and its corresponding time delay is $\tau_J + T/(M-1)$. Then, the coarse estimation of time delay $\tilde{\tau}_J$ can be obtained.

Next, we further precisely estimate the time delay of jamming signal by following steps:

Step1: Search P adjacent range bins around $\tilde{\tau}_J$, and separately assume them as the realistic time delay of jamming signal $\tilde{\tau}_J + \Delta\tau_J^{(p)}$, where $\Delta\tau_J^{(p)} = pT_s$ ($p = -P/2 \sim P/2$).

Step2: Reconstruct the jamming signal $\tilde{J}_{\text{SMSP}}^{(p)}(t)$ under each assumed time delay based on the parameters that have been estimated. Obtain the corresponding canceled mixed signal $y^{(p)}(t) = y(t) - \tilde{J}_{\text{SMSP}}^{(p)}(t)$.

Step3: Calculate the power of jamming and target in $y^{(p)}(t)$ after pulse compression process, and separately denote them as P_j and P_t. When the output JSR (defined as P_j/P_t) minimizes, the corresponding time delay is chosen as the true time delay of the jamming signal, i.e.,

$$\tilde{\tau}_J + \Delta\tilde{\tau}_J = \tilde{\tau}_J + \Delta\tilde{\tau}_J^{(\bar{p})}, \quad \bar{p} = \arg\min_p P_j^{(p)}/P_t^{(p)} \tag{32}$$

4.4 Jamming reconstruction and suppression

According to the estimated results, the jamming signal $\tilde{J}_{\text{SMSP}}(t - \tilde{\tau}_J - \Delta\tilde{\tau}_J)$ can be reconstructed with the form in (3), and then it can be suppressed by subtracting it from the mixed signal (4).

5 Results and discussion

In this section, we conduct some simulation experiments to illustrate the effectiveness of the proposed method in this paper.

5.1 The performance of parameter estimation

The parameters of the target signal and the SMSP jamming are set as follows. The bandwidth and pulse duration of transmit signal are 10 MHz and 50 us respectively, and the sampling frequency is 20 MHz. The number of sub-waveforms of the SMSP jamming is 5, and the time delay of signal (target echo and jamming signal) is 100 us. The length of rectangular window is 1.6 us.

Figure 3 shows the STFT result of the mixed signal when SNR is 5 dB and the JSR is 10 dB. The jamming signal and the target echo intersect in the time-frequency domain. There are three apparent intersections, while the left two theoretical intersections are located at the beginning and the end of the signal respectively, and cannot form high peaks.

After estimating different parameters and reconstructing SMSP jamming according to the steps which has been given in Section 3, the canceled signal after pulse compression process is shown in Fig. 4. The parameters set in this simulation are more practical with the SNR is − 3 dB and the JSR is 20 dB. For comparison, the pulse compression results of the mixed signal and the target signal which only contains the target echo are also plotted in Fig. 4. Obviously, the target is submerged in the jamming signal without cancellation, and it cannot be detected by the radar. After interference cancellation, the position of the target is very clear. Moreover, the canceled signal is basically coincide with the target echo, which means the SMSP signal is almost suppressed.

We next conduct the estimation performance of the proposed method. The JSRs are separately fixed as 5 dB and 15 dB, and the SNR changes from − 5 dB to 10 dB. The estimation performances of different parameters are shown in Fig. 5. From Fig. 5a, it is easy to find that the number of sub-waveforms can be correctly estimated once the SNR is bigger than 3 dB when the JSR is 5 dB. When the JSR is 15 dB, the number of sub-waveforms can always be correctly estimated. Figure 5b plots the root mean squared error
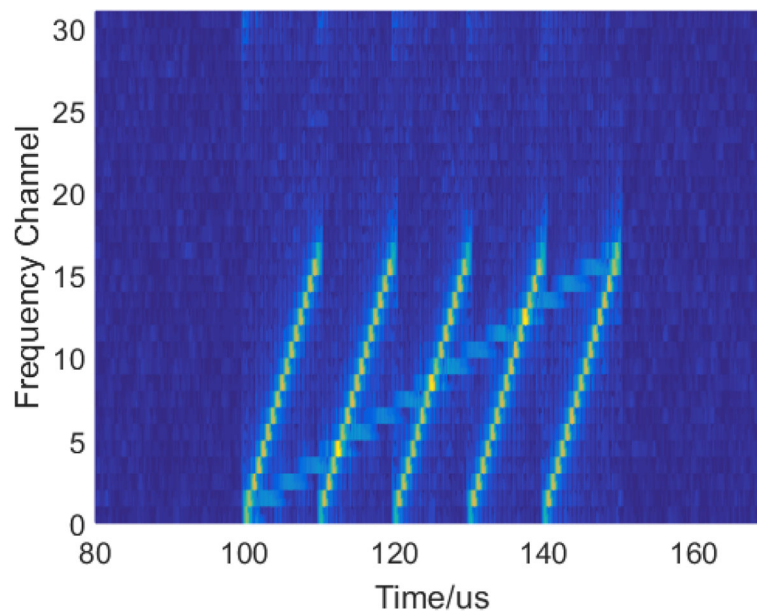

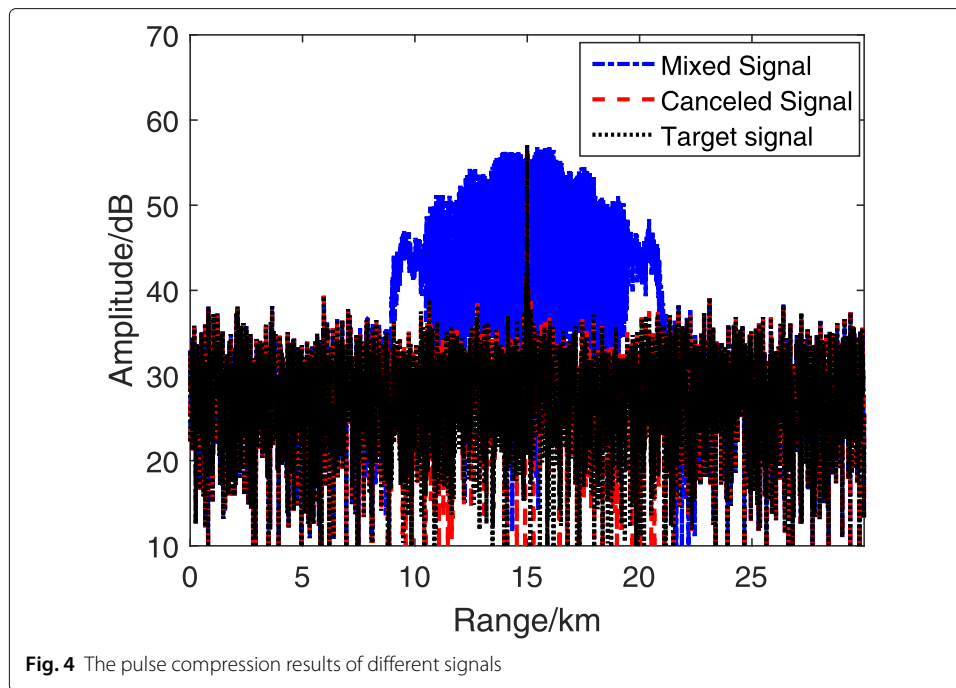**Fig. 3** The STFT result of mixed signal

Fig. 4 The pulse compression results of different signals

(RMSE) of the estimation result of amplitude, and Fig. 5c respectively plots the RMSE of the coarse estimation result and the fine estimation result of time delay. Clearly, the higher JSR and higher SNR, the slower RMSE of parameter estimation, and the better estimation performance. It should be noticed that the RMSE of fine estimation to time delay is always 0, which means the estimated time delay by this method has a pretty high accuracy.
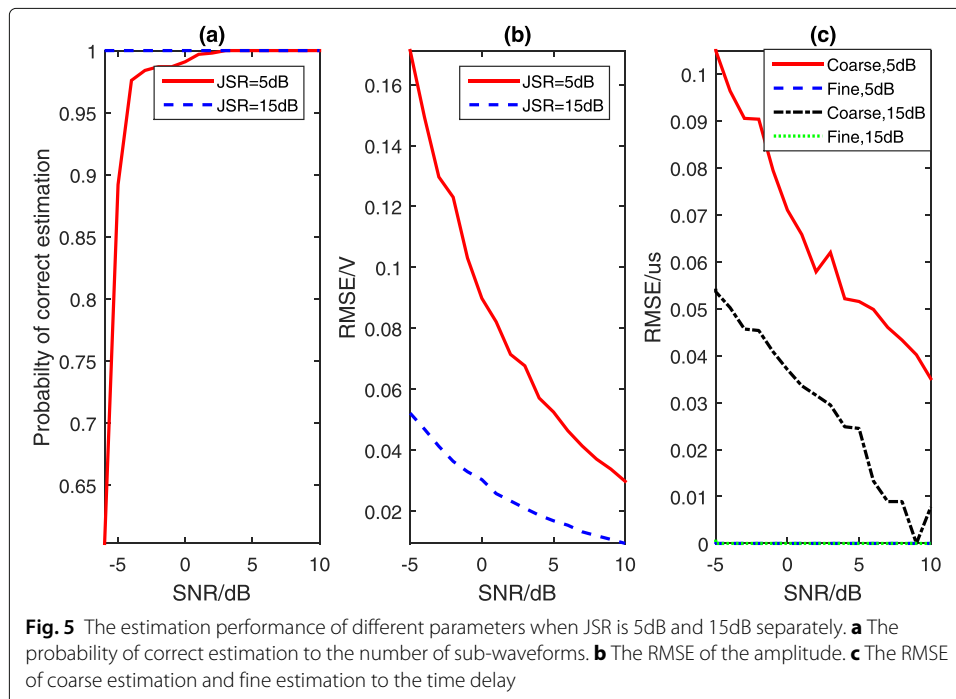
Fig. 5 The estimation performance of different parameters when JSR is 5dB and 15dB separately. **a** The probability of correct estimation to the number of sub-waveforms. **b** The RMSE of the amplitude. **c** The RMSE of coarse estimation and fine estimation to the time delay

Fig. 6 Time domain and frequency domain of different window functions. **a** Time domain. **b** Frequency domain
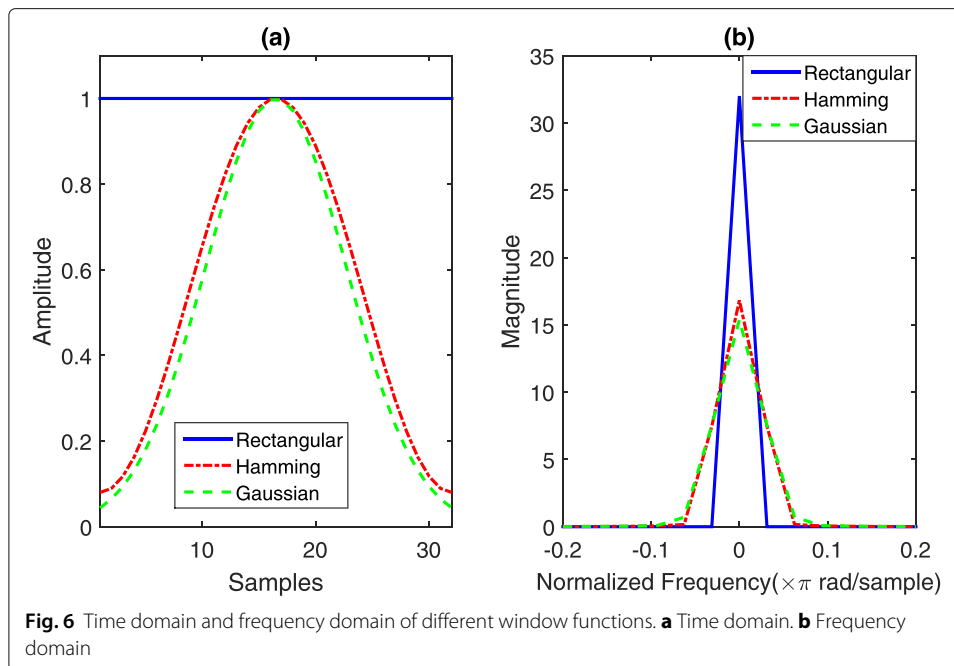
5.2 The performance of jamming suppression

The STFT result with different analysis window may result in different estimated result of amplitude. Here, a Hamming window and a Gaussian window are used for comparison. Figure 6 gives the time domain and the frequency domain of different windows. In Fig. 7, the estimated amplitude with different window is shown. Obviously, the result by using rectangular window coincide exactly with the real value and is always slightly smaller than that by using Hamming window and Gaussian window.

Fig. 7 Estimated value of jamming signal using STFT with different window functions
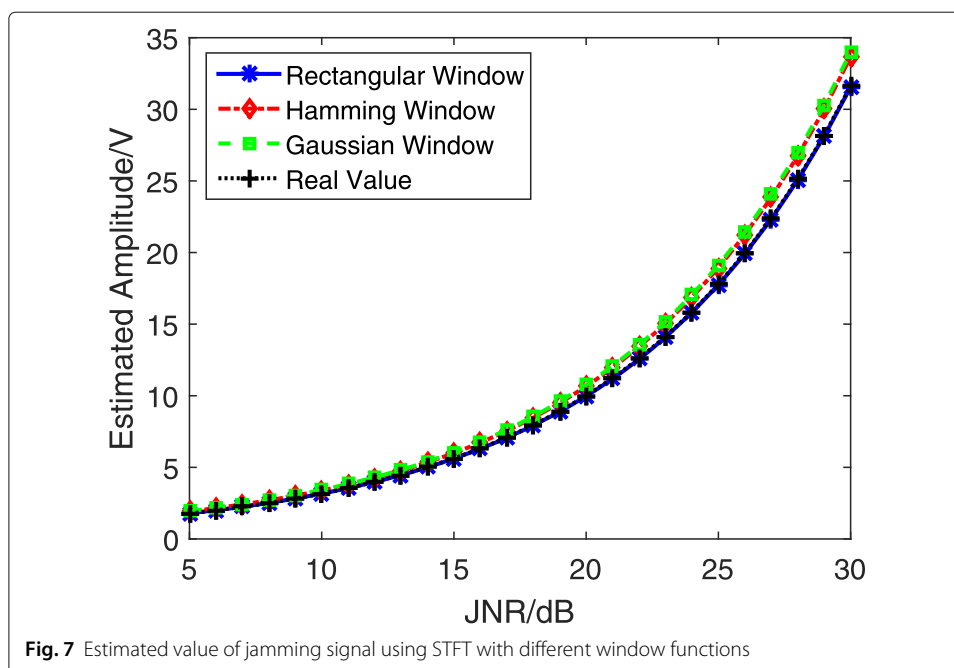
In Fig. 6a, we set the time domain maximum of the three window functions to 1. From Fig. 6b, the peaks of the three main lobes are 32, 16.82, and 15.39 respectively for the spectrum of rectangular window, Hamming window, and Gaussian window. Obviously, the Hamming window and the Gaussian window are almost the same and have a broader main lobe than the rectangular window in their spectrum, while the steps in Section 4.1 only consider the maximum peak value in the main lobe and ignore the energy in the side lobe of the spectrum. Consequently, the estimated amplitude, when choosing the non-rectangular window, is greater than the real value. By comparing the main lobe width of the spectrum of different window functions and the estimated error of amplitude, we can conclude that the wider the main lobe of the spectrum, the more energy is lost and the greater error of amplitude estimation. When the JNR is 30 dB, the estimation errors to amplitude of hamming window and Gaussian window are about 2 dB.

In order to evaluate the performance of jamming cancellation, we use the definition of the jamming suppression ratio $R = JSR_2 - JSR_1$ in [11] and compare the performance with it, where JSR_2 and JSR_1 are the JSR in the canceled signal after pulse compression and in the received mixed signal (before pulse compression) respectively. Set JSR_1 as 5dB, and JNR changes from 5 dB to 30 dB. Both of the curves that the jamming suppression ratio R versus JNR according to the method in [11] and in this paper are plotted in Fig. 8. It can be seen that the jamming suppression ratio R obtained by the proposed method is almost the same as that in [11] when the JNR is low. Due to the extremely high accuracy of the amplitude, our performance is better and better as JNR increases. When JNR is 30 dB, the R in our method is higher about 0.5 dB.

5.3 Discussion

Although the cancellation performance with rectangular window is better when compared to other windows, this result is obtained when the window length is relative short

Fig. 8 Comparison of the jamming suppression ratio with other methods (JSR = 5dB)
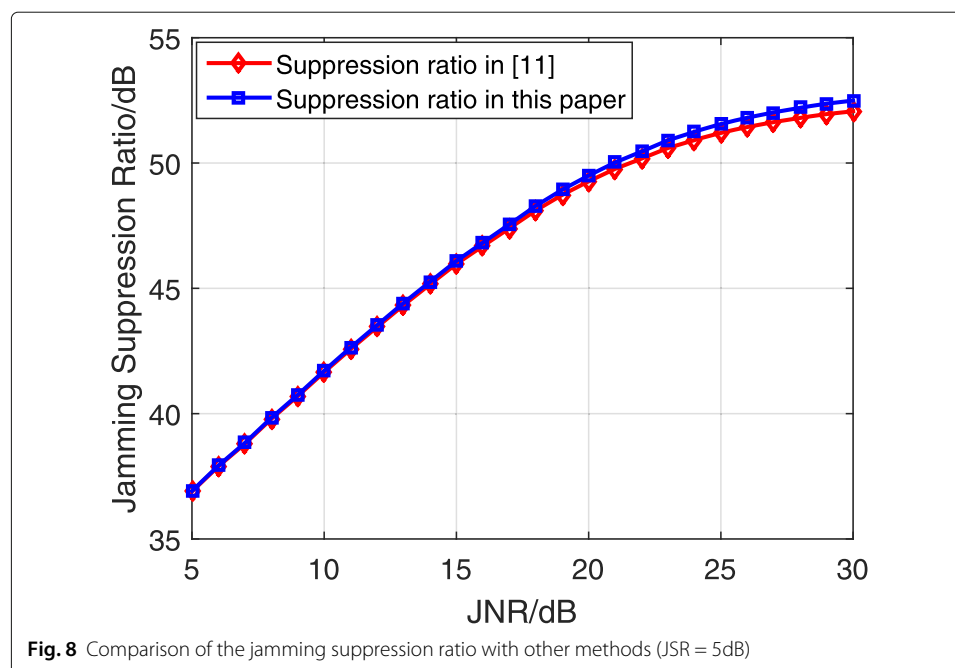
(e.g., 1.6 us). However, when the analysis window is longer, the spectrum of extracted signal with rectangular window becomes smooth, resulting in the approximate expression in (13) which is not fully applicative to estimate the amplitude of jamming signal. In other words, the cancellation performance with the rectangular window may deteriorate under longer window length scenario, even worse than the method in [11].

6　Conclusions

We considered the interference suppression problem of SMSP in the mixed signal received by radar. To this end, we resort to the method of parameter estimation and signal reconstruction. The mathematical expression for the STFT result of the SMSP jamming is derived. Based on this, the different parameters of SMSP jamming are estimated. The number of sub-waveforms are estimated by the times of frequency hops in time duration, which is always correct when JNR is higher than 8 dB. The amplitude is estimated through the modules of the STFT result of the mixed signal. The coarse estimation to time delay is achieved by finding the position where SMSP jamming intersect with target echo in time-frequency domain. By comparing the results of choosing different window functions on the amplitude estimation of the SMSP signal, we find that the narrower the main lobe of the window's spectrum, the more accurate the amplitude estimation of the jamming signal. The numerical simulations illustrate the accuracy of parameter estimation and the effectiveness of jamming suppression through this method. Compared with other methods, its jamming suppression ratio is higher about 0.5 dB when JNR is 30 dB.

References
1. M. J. Sparrow, J. Cikalo, in *United States Patent*, ECM techniques to counter pulse compression radar, (2006). 7081846
2. Y. Li, X. Ying, B. Tang, in *2011 International Conference on Computational Problem-Solving (ICCP)*, SMSP jamming identification based on matched signal transform, (2011), pp. 182–185. https://doi.org/10.1109/iccps.2011.6092274
3. Y. Zhao, D. Du, A. A. Ali, B. Tang, in *2014 IEEE 17th International Conference on Computational Science and Engineering*, Detection of SMSP jamming in netted radar system based on fractional power spectrum, (2014), pp. 989–993. https://doi.org/10.1109/cse.2014.197
4. T. Bu, Y. Dong, G. Wu, W. Xing, A study on technology of recognizing SMSP jamming. Mod. Radar. **37**(2), 42–4574 (2014)
5. Y. Li, G. Lu, B. Tang, Jamming identification algorithms of SMSP and C&I based on ambiguity function. Aero. Weaponry. **0**(04), 51–54 (2011)
6. S. Yang, B. Tian, Identification algorithm of SMSP and C&I. J. Detect. Control. **38**(06), 62–67 (2016)

7.   L. Ding, R. Li, L. Dai, F. Chen, Y. Wang, Discrimination and identification between mainlobe repeater jamming and target echo via sparse recovery. IET Radar. Sonar. Navig. **11**(2), 235–242 (2017)

8.   L. Ding, R. Li, Y. Wang, L. Dai, F. Chen, Discrimination and identification between mainlobe repeater jamming and target echo by basis pursuit. IET Radar. Sonar. Navig. **11**(1), 11–20 (2017)

9.   M. Sun, B. Tang, Suppression of smeared spectrum ECM signal. J. Chin. Inst. Eng. **32**(03), 407–413 (2009)

10.   X. Li, C. Wang, H. Yuan, SMSP jamming suppression method based on jamming reconstruction and kurtosis maximum. J. Beijing Univ. Aeronaut. Astronaut. **44**(06), 63–71 (2018)

11.   H. Yuan, C. Wang, L. An, X. Li, Smeared spectrum jamming suppression method based on signal reconstruction. J. Syst. Eng. Electron. **39**(05), 960–967 (2017)

12.   Y. Lu, M. Li, R. Cao, Z. Wang, J. Chen, Jointing time-frequency distribution and compressed sensing for countering smeared spectrum jamming. J. Electron. Inform. Technol. **38**(12), 3275–3281 (2016)

13.   G. Lu, S. Liao, S. Luo, B. Tang, Cancellation of complicated drfm range false targets via temporal pulse diversity. Prog Electromagn Res C. **16**, 69–84 (2010)

14.   S. C. Pei, J.-J. Ding, Relations between Gabor transforms and fractional Fourier transforms and their applications for signal processing. IEEE Trans. Sig. Process. **55**(10), 4839–4850 (2007)

15.   S. G. Mallat, A theory for multiresolution signal decomposition: the wavelet representation. IEEE Trans. Pattern. Anal. Mach. Intell. **11**(7), 674–693 (1989)

16.   M. Portnoff, Time-frequency representation of digital signals and systems based on short-time Fourier analysis. IEEE Trans. Acoust. Speech Sig. Process. **28**(1), 55–69 (1980)

17.   P. Zan, Y. Liu, M. Chang, Research of rectal dynamic function diagnosis based on FastICA-STFT. IET Sci. Meas. Technol. **12**(8), 965–969 (2018)

18.   L. Bo, L. Luo, Y. Yu, K. Soga, J. Yan, Dynamic strain measurement using small gain stimulated Brillouin scattering in STFT-BOTDR. IEEE Sensors J. **17**(9), 2718–2724 (2017)

19.   K. Binhee, S.-H. Kong, S. Kim, Low computational enhancement of STFT-based parameter estimation. IEEE J. Sel. Top. Sig. Process. **9**(8), 1610–1619 (2015)

20.   S. Neemat, O. Krasnov, A. Yarovoy, An interference mitigation technique for FMCW radar using beat-frequencies interpolation in the STFT domain. IEEE Trans. Microw. Theory Tech. **67**(3), 1207–1220 (2019)

21.   B. R. Mahafza, *MATLAB simulations for radar systems design*. (CRC Press, Florida, Boca Raton, 2003)

Publisher's Note